ENC-2020-0103

NUMERICAL SIMULATION OF A FOUR CYLINDER, FOUR STROKE SPARK IGNITION ENGINE USING ETHANOL / GASOLINE BLENDS

Laura Tatiana Meneses Barrera

laura.meneses@labmci.ufsc.br

Mechanical Engineering - Francisco de Paula Santander University - IM/FI/UFPS.

Avenida Gran Colombia No. 12E-96 Barrio Colsag, San José de Cúcuta, NS, Colombia.

Internal Combustion Engines Laboratory - Joinville Technological Center - Federal University of Santa Catarina - LABMCI/CTJ/UFSC.

Rua Dona Francisca 8300, Joinville, SC, CEP 89219-600, Brazil.

Meimer Peñaranda Carrillo

meimerpc@ufps.edu.co

Mechanical Engineering - Francisco de Paula Santander University - IM/FI/UFPS.

Avenida Gran Colombia No. 12E-96 Barrio Colsag, San José de Cúcuta, NS, Colombia.

Leonel R Cancino

leonel.cancino@labmci.ufsc.br

Internal Combustion Engines Laboratory - Joinville Technological Center - Federal University of Santa Catarina - LABMCI/CTJ/UFSC.

Rua Dona Francisca 8300, Joinville, SC, CEP 89219-600, Brazil.

Abstract. *In this work, a spark-ignition internal combustion engine (SI-ICE) was numerically analyzed using 0D and 1D models in AVL-BOOST™ , using five ethanol-gasoline blends (E0, E20, E40, E60, E84) as fuels. The analysis included varying the compression ratio (CR) of each blend (11, 12.5, 13, 14) by analyzing engine performance and exhaust gas composition parameters, efficiencies, in-cylinder temperatures and pressure. A brief economic feasibility analysis for blends that showed similar power data was also performed. The combustion model used was the Wiebe model, taking the function parameters from the literature. There was a 17% decrease in torque and power for the E84 blend compared to the gasoline at compression ratio of 11. Blends such as E20 with a compression ratio of 13 and E40 with a compression ratio of 14 obtained torque and power values similar to gasoline. The lower heating value of ethanol implies a higher fuel specific consumption; there was a 9.7% decrease in consumption of E84 at compression ratio of 14 compared to E84 at compression ratio of 11.*

Keywords: *Ethanol / gasoline blends, AVL BOOST™ , Spark-ignition internal combustion engines*

1. INTRODUCTION - THE USE OF ETHANOL AS A BLEND IN AUTOMOTIVE FUEL

Despite multiple benefits that the development of internal combustion engines has carried in the transport area, they have also caused important problems for public health and the environment in terms of environmental pollution, due to the emission of greenhouse gases and other harmful gases. Solutions have been continually sought to minimize emissions of pollutants and one of the proposals of greatest acceptance and impact has been the use of biofuels (Stratta, 2002). There are different types of biofuels, but for relevance ethanol will be treated. Ethanol (C_2H_5OH or C_2H_6O) is a biofuel that can be obtained from sugar, corn, beet, potato, etc., and used with gasoline in the spark ignition engines called flex-fuel engines. The ethanol and ethanol / gasoline blends have received great attention as alternative fuels due to the reduction of greenhouse gas emissions and because it is produced from renewable sources (da Silva Jr. *et al.*, 2019), (Cancino *et al.*, 2011). Although it is an attractive biofuel, the hydroxyl group OH incomplete combustion causes high emissions of aldehydes. The aldehydes are highly reactive compounds involved in complex chemical reactions in the atmosphere. The aldehydes considered pollutants are those found in the gaseous state: acetaldehyde (C_2H_4O) and formaldehyde (CH_2O), which are toxic and have harmful effects on health, reaching highly toxicity and potentially carcinogenic (Zaránte and Sodre, 2016). Currently, different countries use ethanol as an additive to gasoline, among which they stand out: United States, Brazil, Canada and the European Union. Brazil is the leading producer of sugar cane-based ethanol, but the United States is the leading producer of ethanol from corn. As for Colombia, Law 693 of 2001 marked the country's entry into the era of biofuels, motivated by the Kyoto Protocol and the dynamics of oil prices (Amaris *et al.*, 2015) and based on environmental sustainability, improved fuel quality, agro-industrial development, employment generation, agricultural

development and energy supply (Monroy and Cepeda, 2016). This law promoted the use of ethanol as an additive to gasoline and introduced certain benefits such as: the exclusion of VAT on sugarcane, the exemption of oil palm income and the control of sales prices of bioethanol and biodiesel (Amaris *et al.*, 2015). In addition to Law 693/2001, Law 939 of 2004 was approved, which also encouraged the use of biodiesel. Subsequently, Decree 4892 of December 23, 2011 ordered the mandatory use of gasoline with 8% ethanol content in those cities with more than 500,000 inhabitants and finally Resolution 40185 established that from 1st March 2018 the ethanol content must be 10%. Because of the above, it is necessary to know the advantages and disadvantages of the use of this biofuel, and therefore, the importance of an adequate combustion of the fuel to avoid emissions of toxic gases and obtain the maximum possible benefits. The aim of this job is to simulate a spark ignition internal combustion engine using five blends as fuel: E0, E20, E40, E60, and E84. The mixtures named above are represented by the letter "E" which indicates that it is a mixture of gasoline with ethanol as biofuel, followed by the volumetric percentage of ethanol in the mixture, therefore, E20 represents a mixture of ethanol and gasoline with 20% ethanol and 80% gasoline (vol.%). The commercial program AVL-BOOST™ was used for simulation purposes. Based on this simulation, the engine operating / performance parameters as well as emissions of CO, CO_2 and NO_X, among other pollutant gases present in the combustion of ethanol were analyzed.

2. METHODOLOGY

The commercial software AVL BOOST™ was used for all numerical simulations. A virtual internal combustion engine was then used in order to numerically investigate the effect / response when ethanol / gasoline blends are used as fuel. The engine model is a four-cylinder spark ignition and for this simulations it was necessary to define operating parameters of the different elements of the engine model, such as the combustion model, fuel properties, among others.

2.1 The 0D model engine used for simulations

The engine model used was taken from the AVL-BOOST™ database and is shown in Figure 1. This model contains the main components of a four-cylinder spark ignition engine, showing the connections between them, four cylinders (C1, C2, C3 and C4) with port fuel injection – PFI type (I1, I2, I3 and I4 are the fuel injectors).
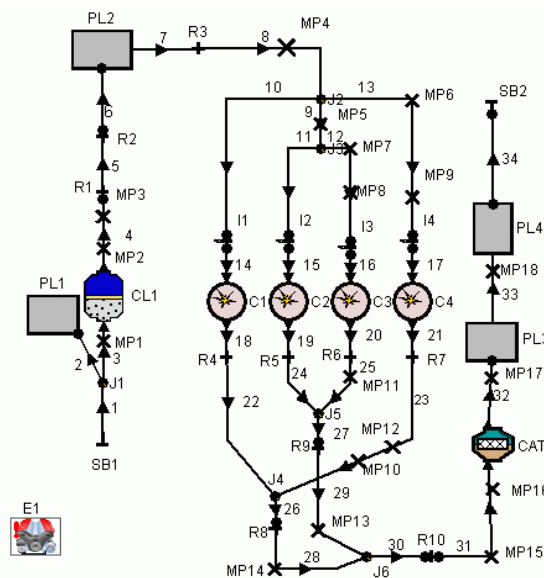

Figure 1. Zero dimensional engine model used in this work

The model has several plenums with different functions, the plenum 2 (P2) is placed intake manifold and plenums 3 and 4 (PL3 and PL4) are placed in the exhaust manifold. The air intake system pursues an air filter (CL1), and the exhaust collector pursues an catalytic converter (CAT1) that for this simulation purposes only takes in to account the pressure lost throughout the exhaust system (no catalytic process is present in the simulation). The system boundaries, i.e. the inlet and outlet of the engine gases represent the system limits (SB1 and SB2). The model also is composed by pipes connecting the above elements, pipe joints, restrictions representing changes in the cross section and several measurement points. It is important to notice that each component in the virtual engine must be defined and set-up data as geometric characteristics, heat transfer as well as pressure lost are necessary. To completely define the simulation, essential parameters must be entered both at the general level and in each of the elements shown in Figure 1. It is important to determine that simulation was "cycle simulation" type, the species transport was "general" mode and additionally where included the

following chemical species in order to better understand the engine emissions: C_8H_{15} (gasoline), C_2H_5OH (ethanol), O_2, N_2, CO_2, H_2O, CO, H_2, O, OH, H, HO_2, H_2O_2, N, NO, N_2O, CH_2O, CH_3HCO, C_2H_4O1-2, CH_3, HCO, CH_2OH, CH_3O, CH_3OH, C_2H, C_2H_2, C_2H_3, CH_2CO. Note that, the approach for species emissions was performed throughout chemical equilibrium and not by chemical kinetics. Simulations were performed at steady state with engine at 2500 rpm. Additionally, the value of the friction mean effective pressure (FMEP) that defines the friction losses was determined using data provided by AVL-BOOST™ , because this parameter despite being of great importance, it is very difficult to find any reference value at literature. In the cylinder, its geometry, valve behavior and the models for combustion and heat transfer were defined. Elements such as the plenums, air filter and catalyst were defined by means of geometry, friction and flow coefficients. Finally, the necessary parameters for injectors, boundary systems, seals, restrictions and pipes were also defined in the simulation set-up.

2.2 The ethanol/gasoline fuel blends properties

Table 1 shows the necessary properties to set-up the fuel blends in the virtual engine used for simulations. The simulated ethanol / gasoline blends were E0, E20, E40, E60 and E84, and their specific properties of heat capacity and stoichiometric air / fuel ratio were then set using the "Gas properties tool" of AVL-BOOST™ for each mixture. The heat capacity of mixtures was determined by the mass percentage of ethanol and gasoline in the blend. Stoichimetric calculations as shown in Heywood (1988) were performed for the air / fuel ratio of each blend.

Table 1. Properties of ethanol / gasoline blends used for simulations

Blend	Lower Heating Value [kJ/kg]	Stoichiometric A/F-Ratio [-]
E0	43529.29	14.60
E20	40133.37	13.396
E40	36864.56	12.23
E60	33715.88	11.11
E84	30086.88	9.82

2.3 Engine heat transfer models and Valve timing

Numerically on AVL-BOOST™ the ports connected to the cylinder must be controlled by an element: by the valve or by the piston. AVL-BOOST™ specifies that the control by the piston is only for 2-stroke engines, therefore the port control by the valve is selected. The inlet valve opening (IVO) occurs 20° before top center (TDC), this point does not have a great influence on the engine performance but it must be ensured that it happens before the TDC to avoid an early pressure drop in the intake stroke. The inlet valve closing (IVC) occurs 70° after bottom center (BDC) in order to provide a superior filling time, although if the intake conditions and pressure differences are not correct it can cause backflow. The exhaust valve opening (EVO) occurs 30° before the bottom center (BDC), i.e., even during the expansion stroke, in order to reduce the cylinder pressure and help to expel the exhaust gases. The exhaust valve closing (EVC) occurs 30° after top center (TDC), the closing happens sufficiently later to guarantee the total exit of the gases. Late EVC favors high power at the expense of low-speed torque and idling. Then, it can be observed that there is an 50° valve overlap period for the inlet and exhaust process. Heat transfer in the cylinder head, piston and the cylinder liner was calculated using the model of Woschni 1978 model ((Lakshminarayanan and Agarwal, 2020), pag. 377), available in AVL-BOOST™ . The surface area and wall temperature of each heat transfer device (piston, cylinder head and liner) was then specified. For the wall temperature of the liner the temperatures in TDC and BDC of the piston were set. Additionally, in the process of gas exchange it is necessary to consider heat transfer due to the high heat transfer coefficient and temperature in the region of the valve and valve seat of the exhaust port. For this, the modified Zapf heat transfer model (Zapf, 1969) was used. All wall temperatures were set following the reference data and recommendations found at AVL-BOOST™ Documentation.

2.4 The Wiebe functions for ethanol / gasoline blends - Experimental data from literature

In 1970 Wiebe developed an expression considering the kinetics of reactions that relates the amount of heat delivered to the total amount of heat, which is calculated with the mass of fuel inside the cylinder and its lower heat capacity (Merker *et al.*, 2012). The Wiebe function is used to approximate actual heat input values in engines. It is one of the simplest combustion models, relating the amount of heat released with respect to the angle of the crankshaft. It is represented by the following set of equations (AVL-AST™ Documentation R2018b., Merker *et al.* (2012), Heywood (1988)):

$$\frac{dx_b}{d\alpha} = \frac{\alpha}{\Delta\alpha_c} (m+1) \left(\frac{\alpha - \alpha_0}{\Delta\alpha_c} \right)^m \exp\left[-a \left(\frac{\alpha - \alpha_0}{\Delta\alpha_c} \right)^{m+1} \right] \tag{1}$$

$$x_b = \int \frac{dx_b}{d\alpha} d\alpha = 1 - \exp\left[-a\left(\frac{\alpha - \alpha_0}{\Delta\alpha_c}\right)^{m+1}\right] \tag{2}$$

$$dx_b = \frac{dQ}{Q} \tag{3}$$

Therefore, in order to define the Wiebe function, it is necessary to know data such as the combustion start (α_0) and duration ($\Delta\alpha_c$), as well as the m and a parameters, which are obtained through statistical adjustments from experimental in-cylinder pressure curves. Yeliana *et al.* (2008) uses five Wiebe function fitting methods in order to find the best fit the Wiebe function curve to the experimentally obtained Mass Fraction Burn (MFB) data from a single-zone Heat Release Rate (HRR) analysis, using ethanol / gasoline blends. In their conclusions, the best fitting method related the mass fraction burn data with four independent variables: (a) the combustion duration till 90% of the mass fraction burn ($\Delta\alpha_{0-90\%}$), (b) the combustion start point α_0, (c) the form factor of the Wiebe function (m) and (d) the amplitude correction factor of the Wiebe function (b). Note that, once fixed the combustion duration to 0 - 90% of mass fraction burned (MFB), the parameter a takes the value of 2.3026. Also, for the best fit, Yeliana *et al.* (2008) fixed the start of combustion α_0 at the point of ignition (spark advance 10° before TDC). Additionally, the mass fraction burn can be corrected by an amplitude correction factor b, under this conditions Equation 2 can be write as follows:

$$x_b = b\left\{1 - \exp\left[-2.3026\left(\frac{\alpha - \alpha_0}{\Delta\alpha_c}\right)^{m+1}\right]\right\} \tag{4}$$

In this work, the Wiebe combustion model was used. The function parameters α, $\Delta\alpha_c$, m, b and a were took from Yeliana *et al.* (2008), that shows the experimental determination by different methods for different ethanol / gasoline blends. That parameters as well as the typical s-shape graphs of the mass fraction burn for all the ethanol / gasoline blends used in this work can be seen in Figure 2.
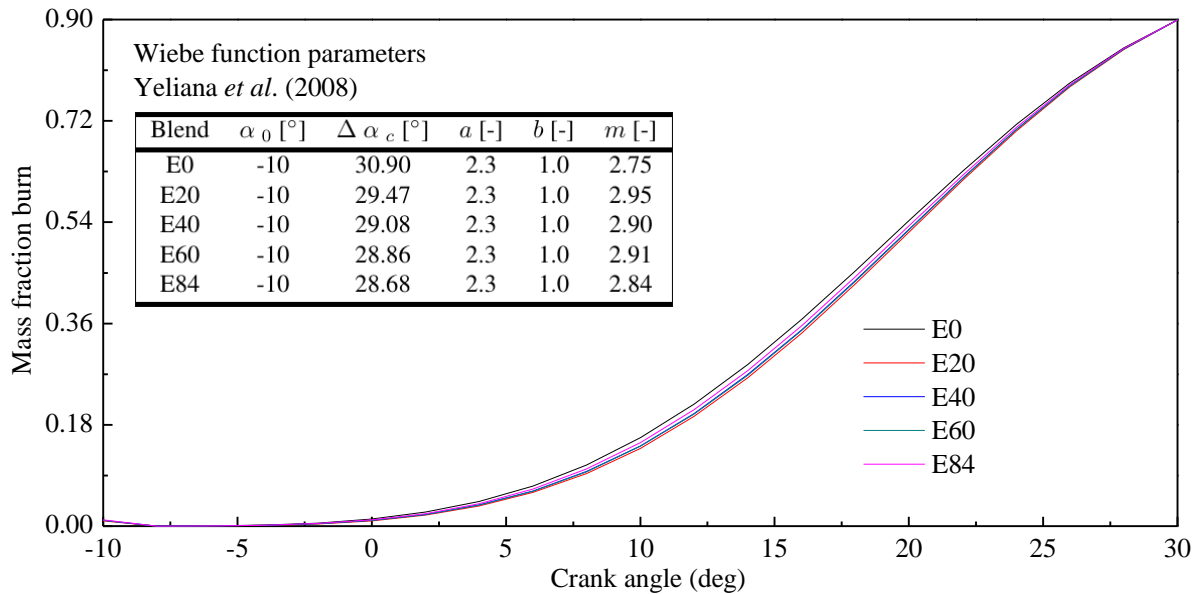

Figure 2. Mass fraction burn profiles for all the blends used in this work - Wiebe function parameters from Yeliana *et al.* (2008)

From Figure 2, it should be noticed that the lower is the ethanol content on the blend, the higher the combustion duration ($\Delta\alpha_c$, defined as 0-90% MFB). Ethanol shows higher laminar flame speed when compared to gasoline (Huang *et al.*, 2015; Del Pecchia *et al.*, 2020) and of this form is normal to expect that any ethanol / gasoline blend burn faster as ethanol content increases in internal combustion engines, under the same operation conditions.

3. RESULTS AND DISCUSSION

The following section shows the results and analysis over the numerical approach of this work. Results are presented in figures always pointed out the simulation conditions in terms of ethanol content (Vol.%) and compression ratio. It is

important to highlight that for pure gasoline (E0) only the simulation at a compression ratio of 11 was taken for analysis purposes, since the results for higher compression ratios do not represent real behavior, since the anti-knock index of gasoline does not allow it to be subjected to high compression ratio values.

3.1 Engine performance parameters

Figure 3 shows the results in terms of power, specific fuel consumption and torque for the virtual engine model of this work. Figure 3(a) shows the engine power for all the cases simulated and the first observation is that engine power will decrease as ethanol content increases and increases as compression ratio increases. Note that the observed decrease is not linear with the ethanol content, for the E84 blend the power drops dramatically, and the specific fuel consumption (Figure 3(b))increases also significantly, when compared to neat gasoline (E0). Figure 3(a) also shows that for E0 and CR11 values of 54 kW were obtained while for E84 to CR14 a power of 47 kW was obtained. In addition, it is observed that the E20-CR13 simulation presents power values very similar to the E0 simulation. For CR11 the power and torque drop between E0 and E84 mixtures is 17%. This indicates that it is not recommended to use high alcohol mixtures with low CR. This is evidenced by the 5.3% gain presented with E84 to CR14 versus E84 to CR11. Finally, from Figure 3(a) it can be seen that E60 to CR14 presents power values only 3% lower than pure gasoline. Figure 3(b) shows the specific fuel consumption (BSFC). It was observed 16% increase between mixtures E0 and E84 to a CR11, while with CR14 and E84 it was 9.7%, the consumption decreased.
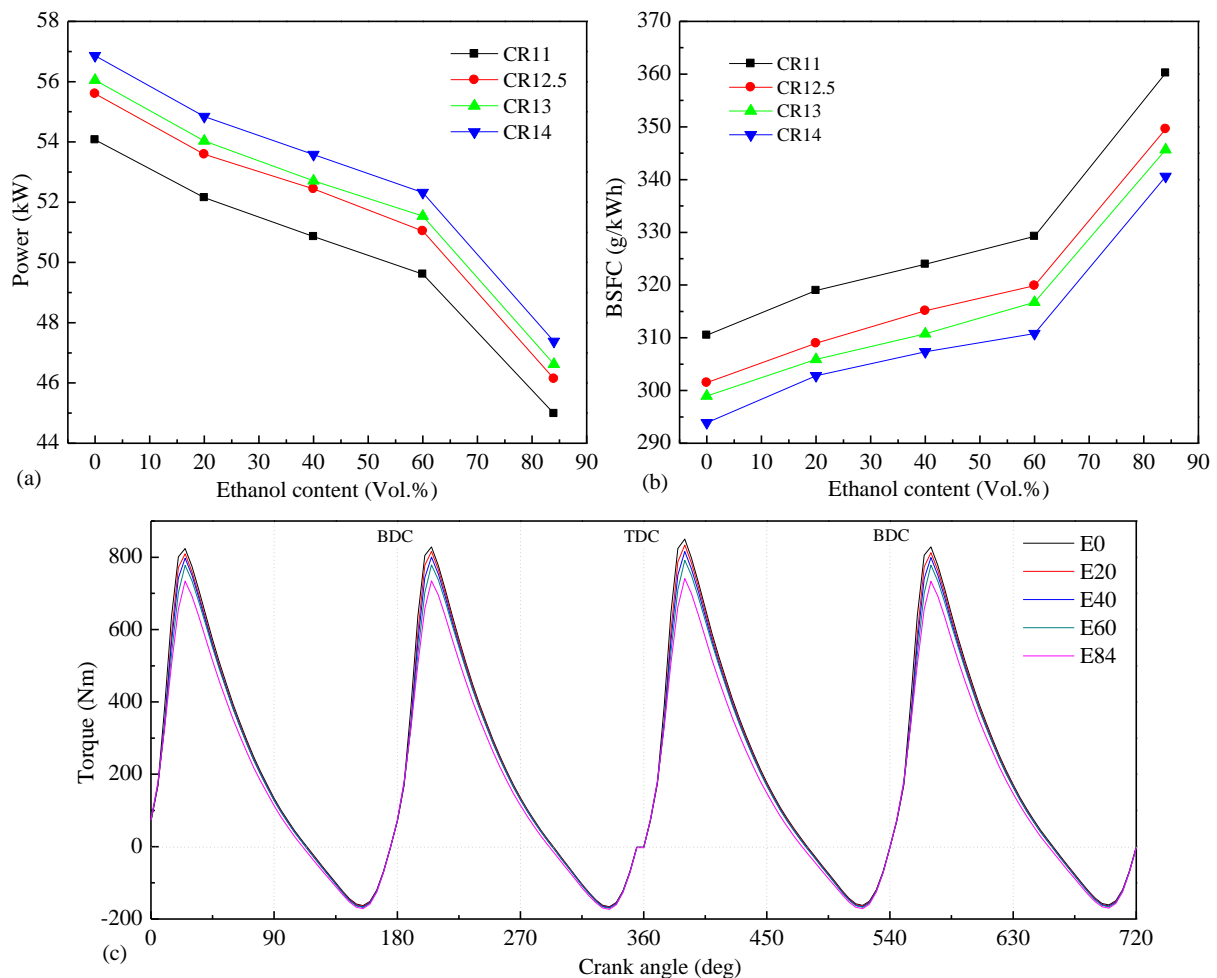

Figure 3. Engine performance parameters: (a) Power, (b) Specific fuel consumption, (c) Torque

Figure 3(c) shows the engine torque for a complete cycle. In this figure it can be seen that the peaks represent the moment when each cylinder reaches its maximum torque, confirming that the torque that is generated by E84 is less than that generated by E0. Additionally, Figure 3(c) shows negative torque values, which are presented due to mass compensation, in the pumping work period. The variation in the torque peaks of each cylinder is due to the difference in the input air and the amount of fuel injected.

3.2 Species mass fractions

In order to analyze the mass composition of the exhaust gases at EVO, Figure 4 (a) is presented, which represents the composition (mass fraction) of combustion products for a compression ratio of 11 and for the different ethanol mixtures simulated (horizontal axis). Initially 28 species were submitted for chemical calculations, but only seven of them are shown, being the species for which the software provided values bigger than zero. Figure 4 (a) shows that the higher ethanol content causes E84 to produce more unburned ethanol (3.8 times more between E84 and E20) and less unburned gasoline. On the other hand,it is observed that H_2O remains constant, while NO increases with ethanol content, which increase 10.6% between E84 and E0. The CO_2, increases, but decreases at E84. Finally, it was observed that CO decreases by 99% between E0 and E84. The calculation made is based on chemical equilibrium, so it was not possible to capture the formation of acetaldehydes and formaldehydes, which implies the need to use chemical kinetics. Figure 4 (b) shows the mass content inside the cylinder for a CR of 11 as function of the crankshaft angle. At 0° the inlet stroke starts, it is observed that the mass is increasing, but then there is a small drop, because the inlet valve closes 70° after the BDC . This causes mass return through the intake duct showing that the valve opening is not the most suitable for the engine speed operation. The amount of mass returned is approximately 5%, i.e. it is determined that the valve timing diagram is not correctly calibrated. It can be seen that the mass in the cylinder is never equal to zero, that remaining mass is the waste gas. A decrease of $2.5x10^{-5}$ kg is calculated for mixture E84 compared to E0. Figure 4 (c) shows the species mass fractions behaviour along the 4 strokes for the E20 mixture with a compression ratio of 11.
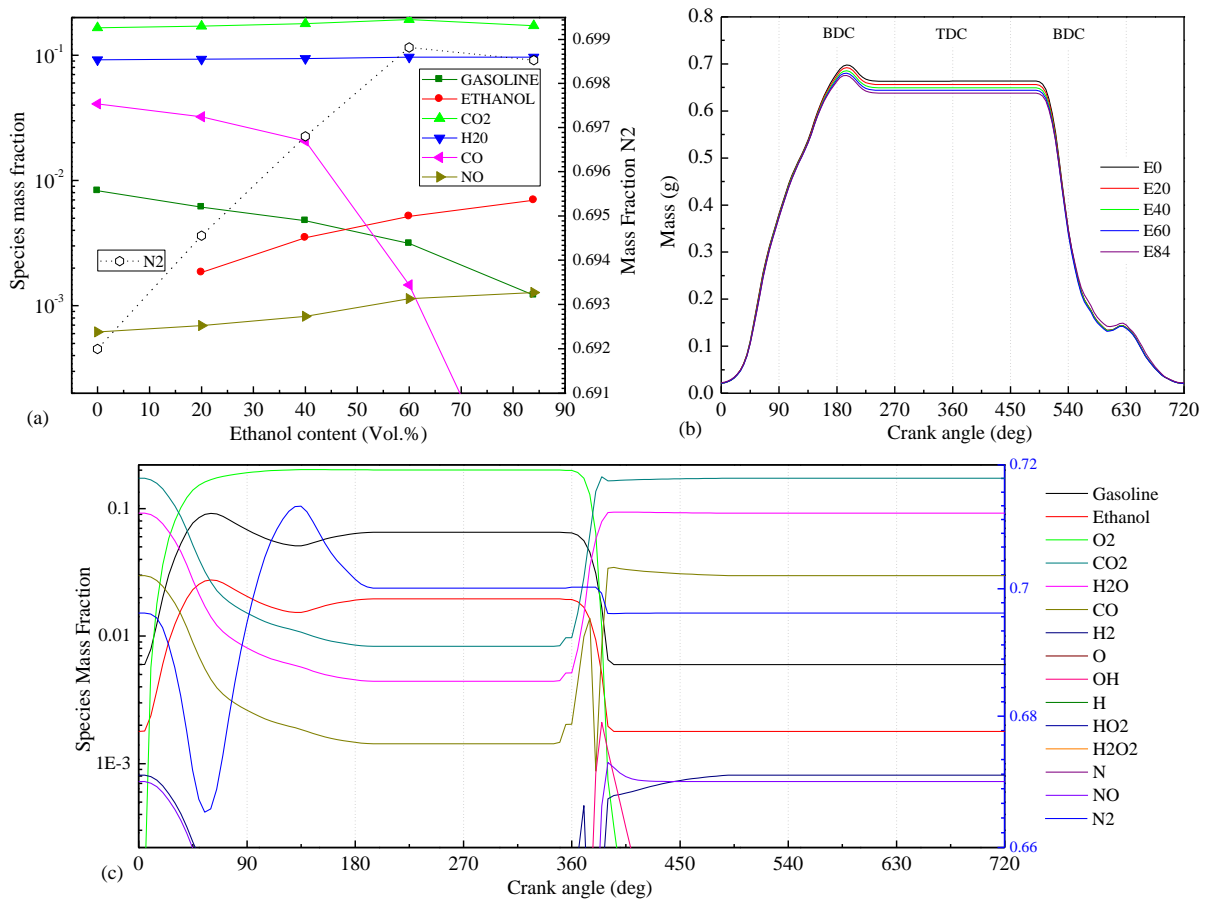

Figure 4. (a) Chemical species for compression ratio = 11 and for all ethanol / gasoline blends (b) In-cylinder mass for compression ratio = 11 and all ethanol / gasoline blends, (c) Chemical species for compression ratio = 11 and E20 blend

3.3 In-cylinder pressure curves

Graphs on Figure 5 shows the in-cylinder pressure curves in function of the crankshaft angle (a) and (b) and sweep volume (c). It should be noted that the results given in BOOST the TDC is taken at 0° but to better observe the results the TDC was moved to 360°. Figure 5(a) shows the pressure behavior for neat gasoline and for all the compression ratios simulated in this work, in the same way, Figure 5(b) shows the results for E84 blend. Comparing both the Figures 5 (a) and (b), it can be seen that the pressure drop between E0 and E84 to CR11 was 19.5% while for E84 and CR14 it was 6.8
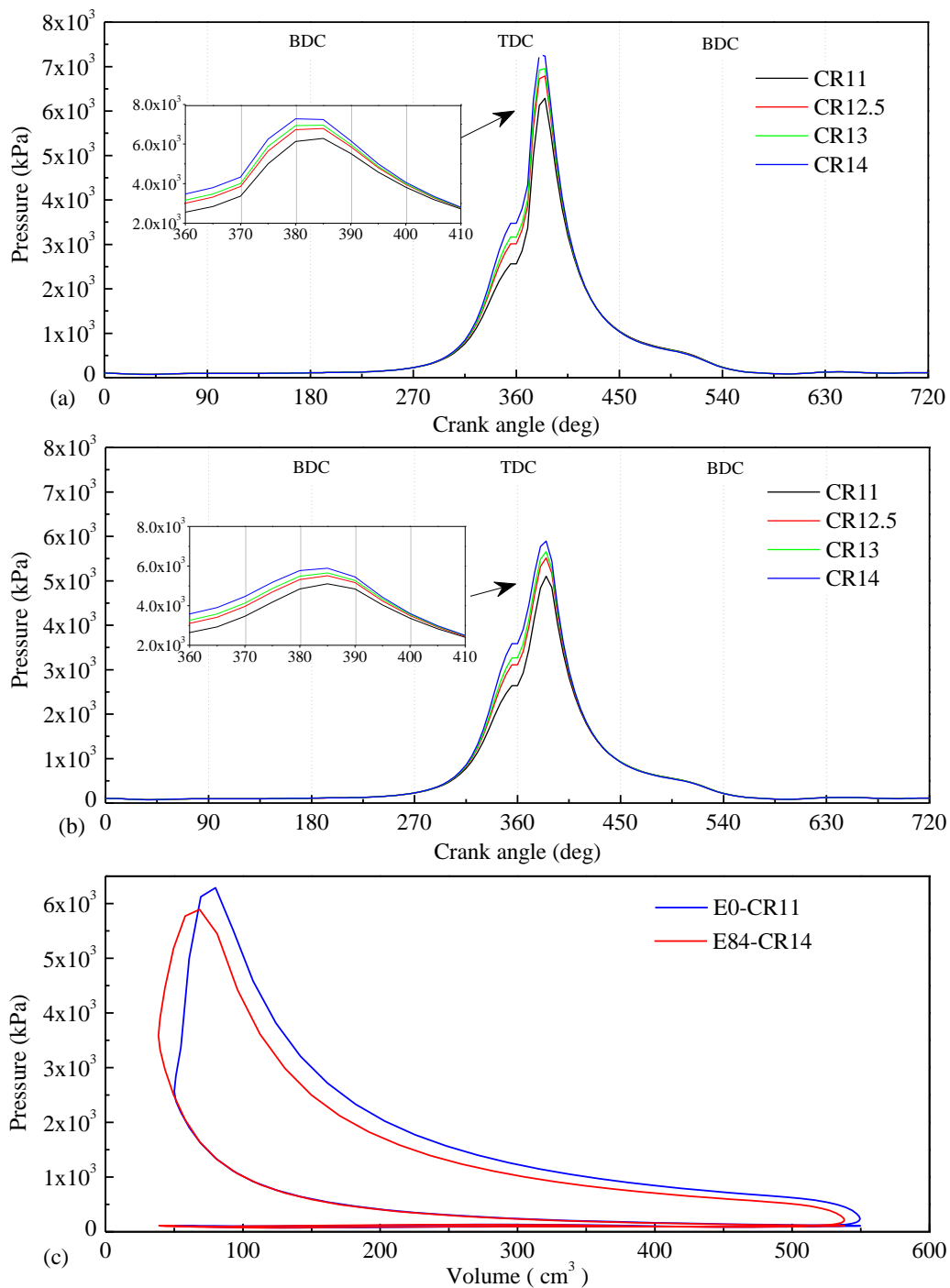
Figure 5. (a) In-cylinder pressure curves for E0 and all compression ratios, (b) In-cylinder pressure curves for E84 and all compression ratios (c) $P - V$ diagram for pure gasoline and E84 blend at compression ratio = 14

On the other hand, Figure 5(c) shows the typical $P - V$ diagram for pure gasoline and E84 blend at the highest compression ratio (CR14). This figure shows the behavior of the Otto cycle and identifies each of the processes carried out, as well as the area difference between both the fuels.

3.4 Fuel conversion and thermal efficiency

Fuel conversion efficiency relates the work done on the energy delivered by a given amount of fuel. Figure 6(a) shows the increase in fuel conversion efficiency with ethanol content and compression ratio for all the blends simulated. For all the cases an efficiency between 29 and 38% was observed, indicating that these efficiencies are low. Comparing gasoline and E84 to CR11 an increase of 27% is calculated and between E84 to CR11 and CR14 an increase of 5%. This indicates

better use of fuel with higher ethanol. Another common efficiency is thermal efficiency, but its value is not provided directly by BOOST, so it was calculated by the work done and the heat released during combustion and is shown in Figure 6(b). Figure 6(b) shows that thermal efficiency decreases with ethanol content and compression ratio, about 1.5% between E0 and E60, but for E84 it shows an increase, reaching values slightly higher than E40, that is, for E84 the engine made better use of the heat released. The increase occurred in meanness of the decrease in both the energy released and the work, since the decrease in heat was in greater proportion than that of work.
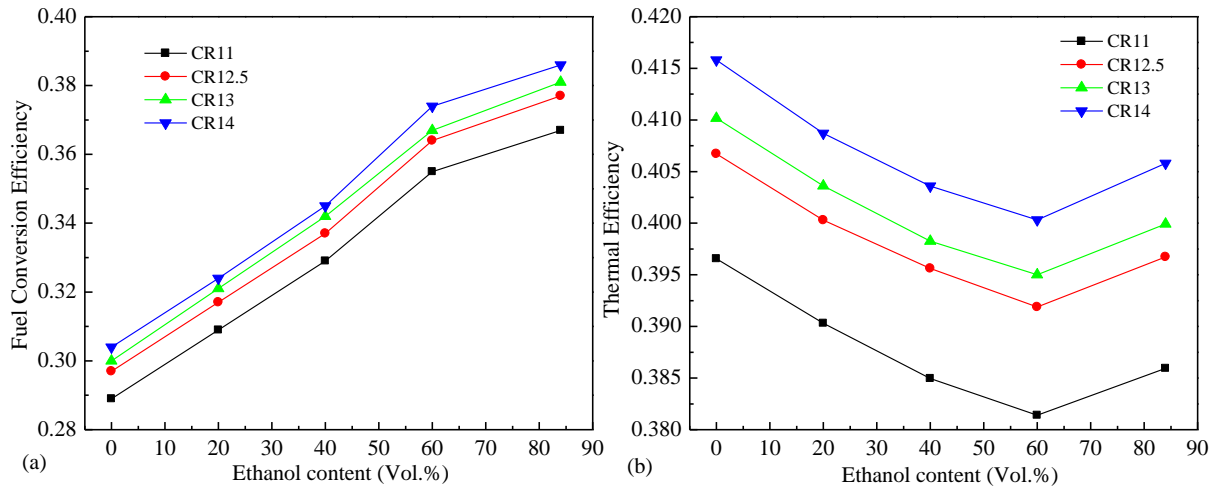

Figure 6. (a) Fuel conversion efficiency and, (b) Thermal efficiency

3.5 In-cylinder temperature and heat transfer

AVL-BOOST™ performs the temperature calculation from the energy conservation and gas state equations. These values depend on several factors such as: fuel mass, heat capacity, fuel evaporation heat, cylinder pressure, heat loss, among others. Figure 7(a) shows the temperature behavior with respect to the crankshaft angle for E0 and for all compression ratios. It can be seen that temperature increases during the compression stroke, reaching its maximum peak at the point where the "combustion process" occurs. Then, it decreases in the expansion stroke and during the exhaust gases exit, presenting a slight increase near 640 ° , this can be caused by the reaction of unburned hydrocarbons with other elements. AVL-BOOST™ also allows to calculate the heat lost in the combustion chamber throughout the heat transfer coefficient calculated using the model by Woschni 1987 (Lakshminarayanan and Agarwal (2020)) Figure 7(b) shows the calculated wall heat transfer for each cylinder in the virtual engine model used in this work. For CR11 between E0 and E84 there is a decrease of 0.21 kJ, and for compression ratio = 14 there is an increase in heat loss of about 14% for all blends.
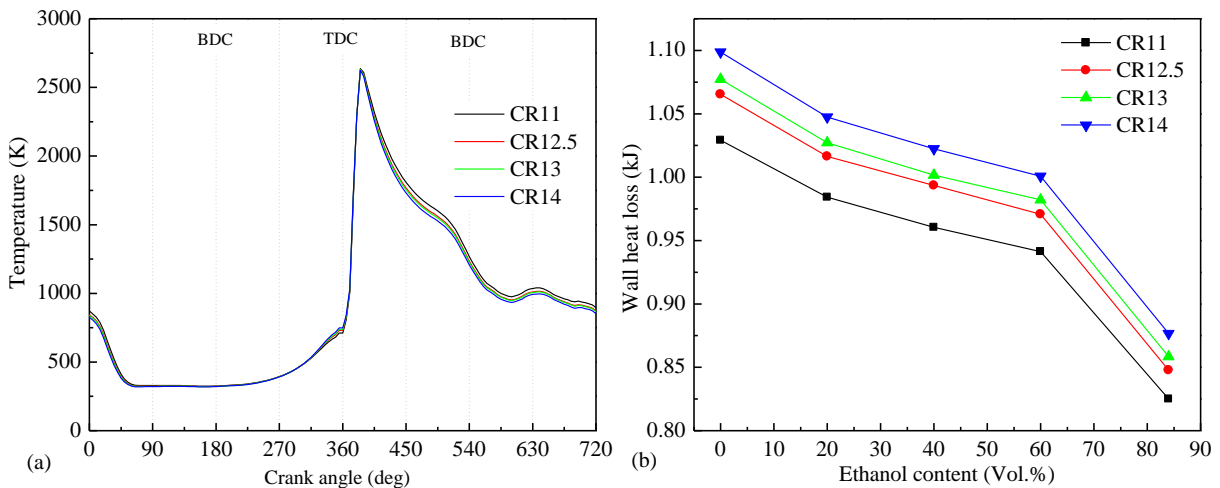

Figure 7. (a) In-cylinder temperature (b) Wall heat loss

3.6 Fuel economy

Finally, a financial analysis of the simulated mixtures is carried out in terms of the power given. Initially, the price of one gallon of each of the blends shown in Table 2 was calculated. The prices were obtained in November 2019, with gasoline in Bogotá (Colombia) at UDS\$ 2.82/gallon and ethanol at USD\$ 2.28/gallon. It was noted then that the gallon of gasoline is USD\$ 0.428 dollar more expensive than the gallon of E84, but as mentioned at the beginning this blend is not yet commercial nor does the transportation fleet have the physical conditions for its use. And as for the used one, it is approximately USD\$ 0.05 dollar less. The savings mentioned above should be analyzed under specific conditions, that is, if the fuel is going to be burned in the same engine as gasoline, there may not really be any economic saving, since the engine does not have the necessary conditions for the correct combustion of ethanol, there will be a higher consumption of fuel that would balance the prices.

Table 2. Cost of 1 gallon of each of the simulated ethanol-gasoline blends

Blend	Gasoline	Ethanol	USD\$ / gallon	Blend	Gasoline	Ethanol	USD\$ / gallon
E0	1.0	0.0	2.82	E40	0.6	0.4	2.61
E10	0.9	1.0	2.77	E60	0.4	0.6	2.50
E20	0.8	0.2	2.71	E84	0.2	0.8	2.39

There are mixture / compression ratio combinations that obtain power values very similar to those of pure gasoline (E0) with a compression ratio of 11, i.e. E20 with a compression ratio of 12.5 and 13 and E40 with a compression ratio of 14. Therefore to determine, from the point of view of fuel cost, whether the use of ethanol is feasible, the cost of producing the indicated power for each of the points taken will be calculated. Table 3 shows the values.

Table 3. Indicated power, work, isfc and total mass for the selected simulations

Blend	Indicated Power (kW)	kWh	isfc (g/kWh)	Mass (kg)
E0-CR11	58.69	7.82E-04	286.06	2.239E-04
E20-CR12.5	58.21	7.76E-04	284.25	2.206E-04
E20-CR13	58.21	7.82E-04	281.78	2.204E-04
E40-CR14	58.21	7.76E-04	282.94	2.196E-04

Table 4 shows the fuel cost required to achieve the specified engine power for each mixture. For approximately the same amount of power, the fuel cost decrease is UDS\$ 0.003¢ per cycle between mixture E0 to CR11 and mixture E40 to CR14. Therefore, it is concluded that, in economic terms, the use of fuel ethanol is feasible, due to its lower price compared to gasoline.

Table 4. Fuel cost required to achieve the specified engine power for each blend and compression ratio

Simulation case	Gasoline (Vol. Gallons)	Ethanol (Vol. Gallons)	USD\$
E0-CR11	8.213E-05	0.000E+00	0.023¢
E20-CR12.5	6.354E-05	1.586E-05	0.021¢
E20-CR13	6.347E-05	1.584E-05	0.021¢
E40-CR14	4.656E-05	3.100E-05	0.020¢

4. CONCLUSSION

In this work, a numerical analysis of a virtual SI-ICE operating with ethanol/gasoline blends was performed using 0D and 1D models in AVL-BOOST, using five ethanol-gasoline blends (E0, E20, E40, E60, E84) as fuels, varying the CR of each blend (11, 12.5, 13, 14) and operating at steady state in 2500 rpm. The results shows that torque and power decrease for higher concentrations of ethanol in gasoline and increase as cylinder compression ratio increases. It was observed 17% decrease in torque and power for the E84 mixture compared to neat gasoline. In turn, blends such as E20 at a compression ratio of 13 and E40 at a compression ratio of 14 obtained torque and power values similar to those of gasoline, demonstrating that it is possible to improve the performance of biofuels if they are burned under specific conditions suitable for better improve the combustion process. The lower heating value of ethanol implies higher fuel specific consumption, the higher the ethanol content in the blend, the higher the fuel consumption. For the E84 mixture there was an increase of around 16% of the BSFC compared to gasoline, decreasing to 9.7% if the E84 mixture is burned

at a compression ratio of 14. There are also alternative mixtures that compare the BSFC of gasoline: E20 to CR12.5, E40 to CR13, and E60 to CR14. AVL-BOOST™ did not capture the formation of formaldehydes and acetaldehydes because the internal calculations of species mass fractions at the exhaust gases were carried out via chemical equilibrium. It would be necessary to use detailed chemical kinetics for the numerical determination of this kind of emissions. The price per gallon of gasoline with respect to the E84 blend would be USD$ 0.428 dollar more expensive, due to the subsidized price of ethanol in the country. The mixture of regulated gasoline in E10 and under the methodology used for the approximate calculation of a market price, acquiring a gallon of this type of fuel means a saving of USD$ 5.34¢ for users. Specific combinations of ethanol content and compression ratio achieve power values similar to those of gasoline: E20-CR12.5, E20-CR13, and E40-CR14. With these mixtures, yields equivalent to those of gasoline are achieved with lower fuel costs. From the literature review, it is concluded that automobiles in Colombia do not have the necessary capabilities to burn ethanol properly, which could present economic problems, physical damage to automobiles and an increase in the concentration of emissions of aldehydes and nitrogen oxides despite the decrease in CO_2 and CO.

5. ACKNOWLEDGEMENTS

6. REFERENCES

Amaris, J.M., Manrique, D.A. and Jaramillo, J.E., 2015. "Biocombustibles líquidos en Colombia y su impacto en motores de combustión interna. Una revisión". *Fuentes, el reventón energético*, Vol. 2, pp. 23–34. doi:10.18273/revfue. v13n2-2015003.

Cancino, L., Fikri, M., Oliveira, A. and Schulz, C., 2011. "Ignition delay times of ethanol-containing multi-component gasoline surrogates: Shock-tube experiments and detailed modeling". *Fuel*, Vol. 90, No. 3, pp. 1238 – 1244. doi: 10.1016/j.fuel.2010.11.003.

da Silva Jr., A., Hauber, J., Cancino, L. and Huber, K., 2019. "The research octane numbers of ethanol-containing gasoline surrogates". *Fuel*, Vol. 243, pp. 306 – 313. ISSN 0016-2361. doi:10.1016/j.fuel.2019.01.068.

Del Pecchia, M., Pessina, V., Berni, F., d'Adamo, A. and Fontanesi, S., 2020. "Gasoline-ethanol blend formulation to mimic laminar flame speed and auto-ignition quality in automotive engines". *Fuel*, Vol. 264, p. 116741. ISSN 0016-2361. doi:https://doi.org/10.1016/j.fuel.2019.116741.

Heywood, J.B., 1988. *Internal Combustion Engine Fundamentals*. McGraw-Hill, New York.

Huang, Y., Hong, G. and Huang, R., 2015. "Numerical investigation to the dual-fuel spray combustion process in an ethanol direct injection plus gasoline port injection (EDI+GPI) engine". *Energy Conversion and Management*, Vol. 92, pp. 275 – 286. ISSN 0196-8904. doi:https://doi.org/10.1016/j.enconman.2014.12.064.

Lakshminarayanan, P.A. and Agarwal, A.K., 2020. *Design and Development of Heavy Duty Diesel Engines A Handbook*. Springer Singapore. doi:10.1007/978-981-15-0970-4.

Merker, G.P., Schwarz, C. and Teichmann, R., 2012. *Combustion Engines Development: Mixture Formation, Combustion, Emissions and Simulation*. Springer, Berlin.

Monroy, C.C.S. and Cepeda, V.L., 2016. "Metodología para el cálculo de energía extraida a partir de biomasa en el departamento de Cundinamarca". Tesis de grado - Universidad Distrital Francisco José de Caldas - Colombia. < http://hdl.handle.net/11349/3687>.

Stratta, J., 2002. "Biocombustibles: los aceites vegetales como constituyentes principales del biodiesel". Bolsa de Comercio de Rosario - Argentina. <https://www.bcr.com.ar/sites/default/files/2018-10/biocombustibles.pdf>.

Yeliana, Y., Cooney, C., Worm, J., Michalek, D. and Naber, J., 2008. "WIEBE FUNCTION PARAMETER DETER- MINATION FOR MASS FRACTION BURN CALCULATION IN AN ETHANOL-GASOLINE FUELLED SI EN- GINE". *Journal of KONES Powertrain and Transport*, Vol. 15, pp. 567–574. URL https://kones.eu/ep2008_3. html.

Zapf, H., 1969. "Beitrag zur untersuchung des wärmeüberganges wärend des ladungswecsels im viertakt-dieselmotor". *MTZ Motortechnische Zeitschrift*, Vol. 30, No. 12, pp. 461 – 465.

Zaránte, P.H.B. and Sodre, J.R., 2016. "Simulation of aldehyde emissions from an ethanol fueled spark ignition engine and comparison with FTIR measurements". *Journal of Physics: Conference Series*, Vol. 745, p. 032023. doi:10.1088/ 1742-6596/745/3/032023.

7. RESPONSIBILITY NOTICE